A helicoidal parametric antenna for subwavelength vortex generation

Noé Jiménez [1], Joao Ealo [2], Rubén Muelas-Hurtado [2], Aroune Duclos [3], Vicent Romero-García [3]

(1) Instituto de Instrumentación para Imagen Molecular (I3M), Universitat Politècnica de València / CSIC, València, Spain

(2) School of Mechanical Engineering, Universidad del Valle, Cali, Colombia.

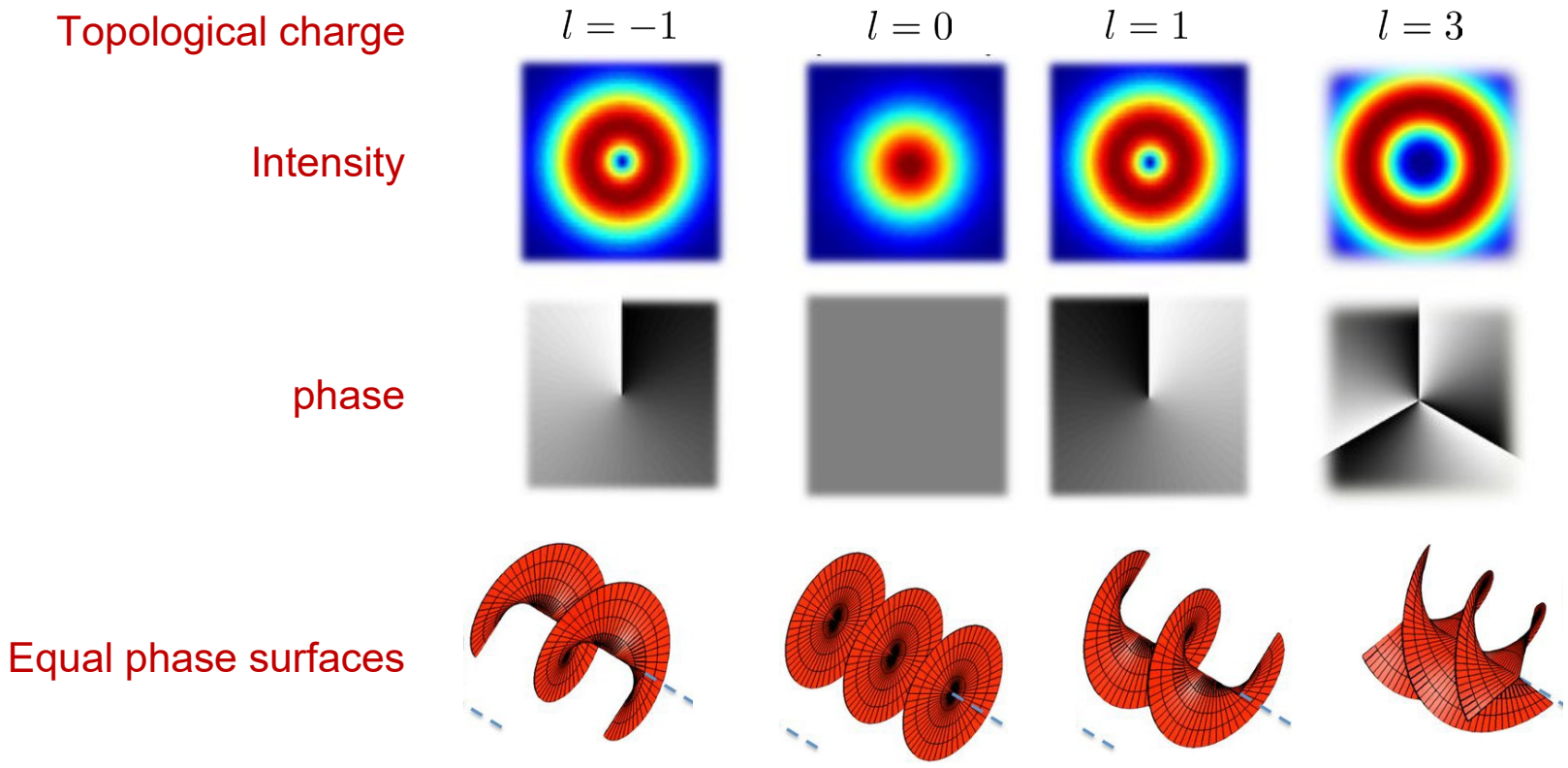
(3) Laboratoire d'Acoustique de l'Université du Mans, CNRS, Le Mans Université, Le Mans, France

22nd International Symposium on Nonlinear Acoustics 2022, July 4th – 8th , 2022

Introduction

Acoustic vortex beams

- Beams presenting a phase dislocation at the axis
- The phase of the field rotates l times with each azimuthal turn



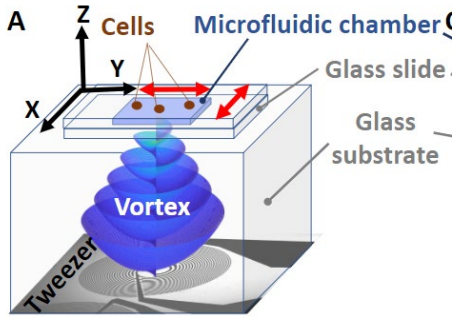
Introduction

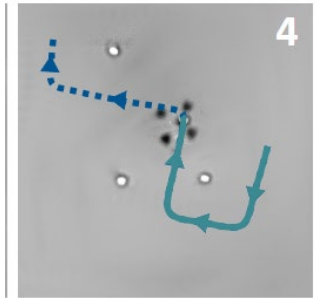
Particle manipulation in biomedical applications

- Guide kidney stones in vivo
- Guide and trap single cells
- Drug delivery: release payload by trapped microbubbles

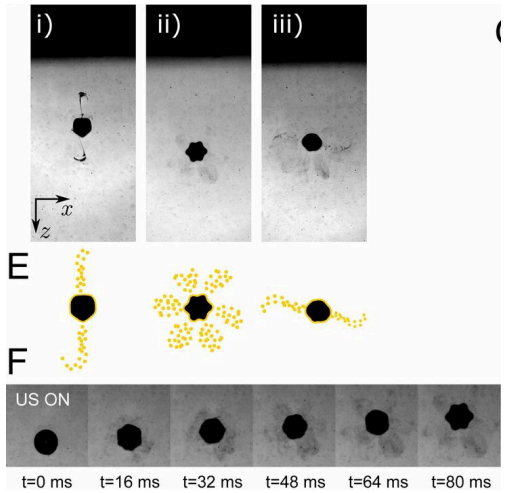


Ghanem, Mohamed A., et al. "Noninvasive acoustic manipulation of objects in a living body." *Proceedings of the National Academy of Sciences* 117(29) 16848-16855 (2020)





Baudoin, M., Thomas, J. L., et al. “Spatially selective manipulation of cells with single-beam acoustical tweezers”. *Nature comm*, *11*(1), 1-10 (2020).



Baresch, D., & Garbin, V. “Acoustic trapping of microbubbles in complex environments and controlled payload release”. *Proceedings of the National Academy of Sciences*, *117*(27) 15490-15496 (2020)

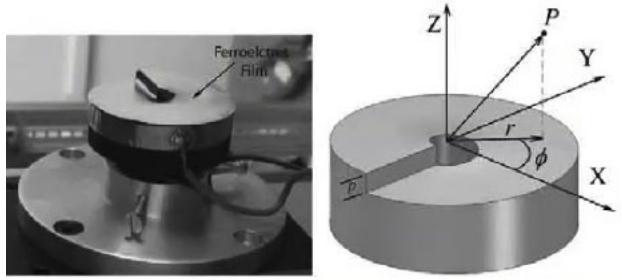
Introduction

Phased-arrays



T Hefner JASA 106, 3313 (1999)
JL Thomas, PRL, 91 244302 (2003)
R Marchiano PRE 71 066616 (2005)
JF Pazos-Ospina JASA 142 61 (2017)

Helicoidal surfaces



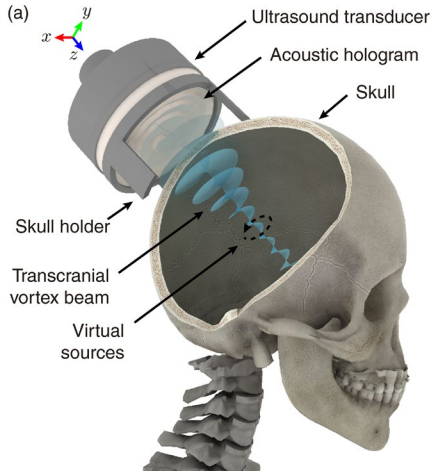
T Hefner JASA 106, 3313 (1999)
L Ealo IEEE 58 1651 (2011)

Spiral gratings



N Jimenez PRE 94 053004 (2016)
T Wang APL 109 123506 (2016)
N Jimenez APL 112 204101 (2018)

Holograms



S. Jiménez-Gambín PRApp 12 014016 (2019)

In all these techniques diffraction limits the size of the vortex

Introduction

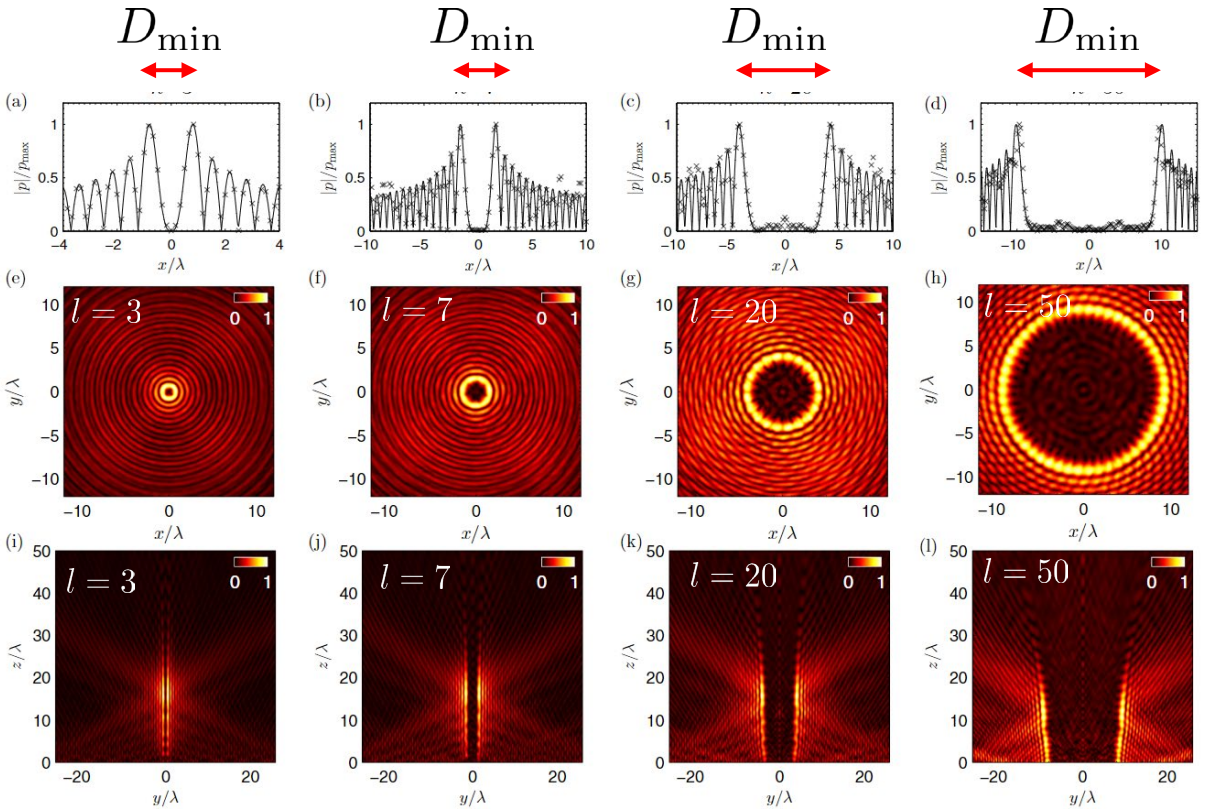
Diffraction-limited vortices

- Bessel beams:
  The radius of the reduced sound areas can be estimated from the position of the first maximum of the n-th Bessel function as [1, 2]

$$D_{\min} \approx \frac{\lambda(|l| + 0.8086|l|^{1/3})}{\pi}$$

- For example, $l = 1$ results in $D_{\min} \approx 0.57\lambda$

- The core width increases with topological charge and distance due to diffraction!



Can we generate a vortex with a core smaller than the wavelength at a large distance?

[1] N Jimenez PRE 94 053004 (2016)
[2] M. Abramowich, Handbook of Mathematical Functions with Formulas, Graphs and Mathematical Tables (Dover, New York, 1972)

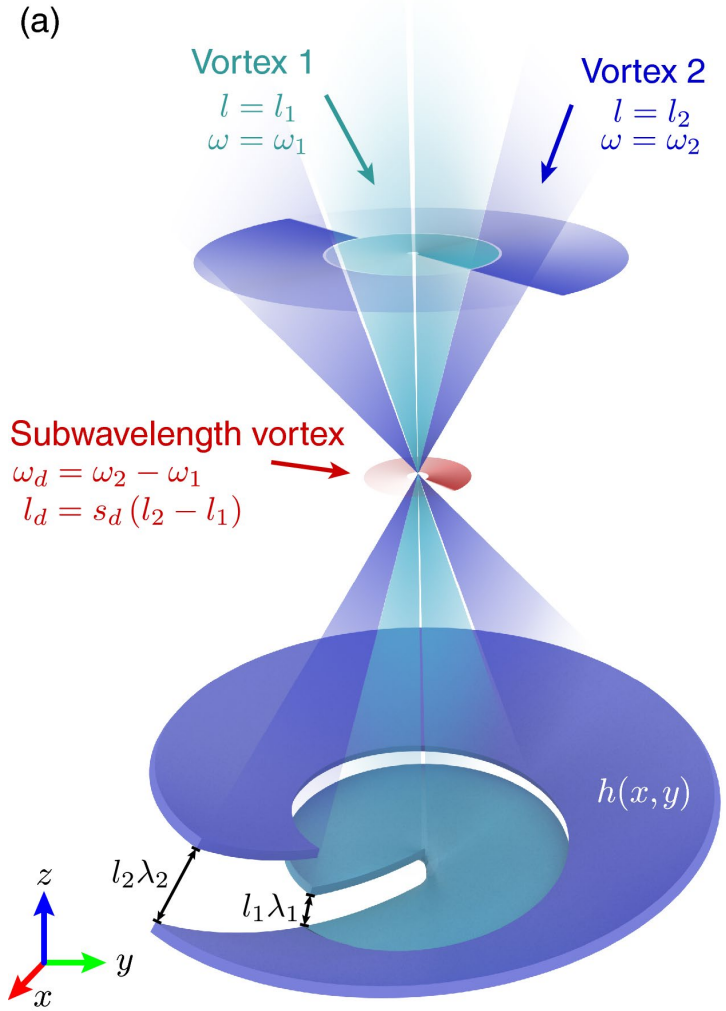
Introduction

Goals of the work

- Generate subwavelength vortices beyond Rayleigh diffraction length

Proposed method

- Use the nonlinear mixing of two confocal, high-frequency and detuned vortex beams of different topological charges
- Subwavelength-vortices will emerge as the natural self-demodulation phenomenon in air
- Vortices can be focused at a distance beyond the Rayleigh diffraction length
- Use an helicoidal focused surface



Methods

Helicoidal surface for focused vortex generation

- The surface should generate a wavefront with a temporal delay

$$\Delta t_n(\phi) = \frac{l_n \phi}{\omega_n},$$

- The radius of the helicoidal surface, in spherical coordinates, is

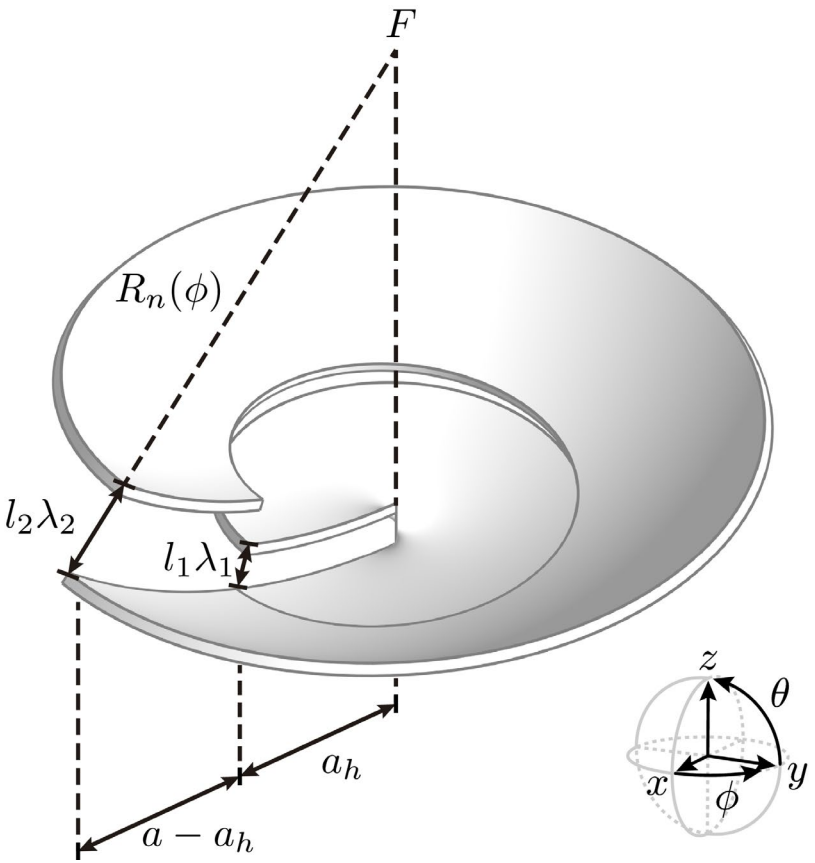
$$R_n(\phi) = F - \frac{l_n \lambda_n \phi}{2\pi},$$

- Finally, the surface coordinates are

$$x_n(\phi,\theta) = R_n(\phi)\cos(\phi)\sin(\theta),$$
$$y_n(\phi,\theta) = R_n(\phi)\sin(\phi)\sin(\theta),$$
$$z_n(\phi,\theta) = -\left[F + R_n(\phi)\cos(\theta)\right],$$

- where $0 < \phi < 2\pi$, and $\theta_{\min}^{[n]} < \theta < \theta_{\max}^{[n]}$
- The aperture angles are given by

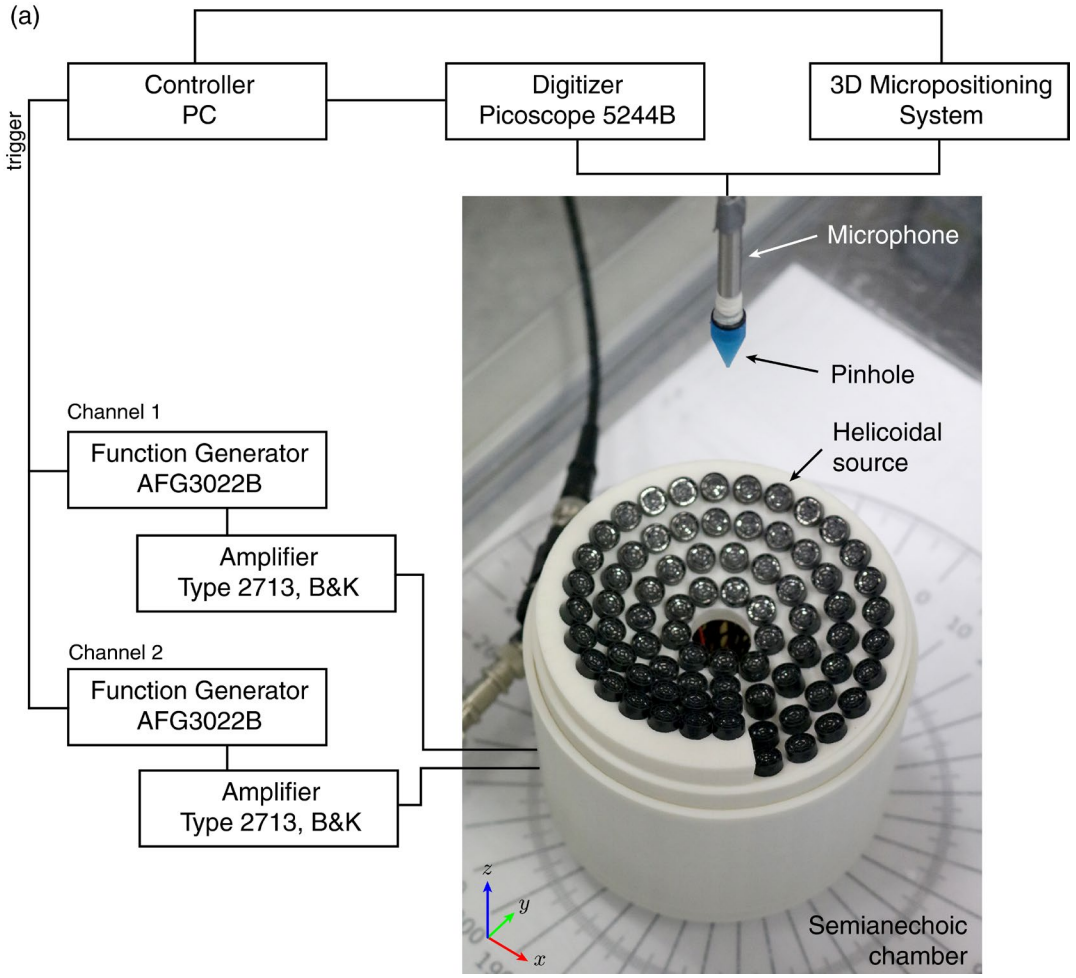
$$\theta_{\max}^{[2]} = \tan^{-1}\left(\frac{a}{2F}\right), \theta_{\min}^{[2]} = \tan^{-1}\left(\frac{a_h}{2F}\right), \quad \theta_{\max}^{[1]} = \theta_{\min}^{[2]}, \theta_{\min}^{[1]} = 0,$$



Methods

Helicoidal surface for dual vortex generation

- Two concentric arrays of transducers (N = 74)
- Total source aperture was 2a = 110 mm (ah = 60 mm)
- Piezoelectric transducers (MA40S4S), OD = 10 mm
- Two arrays (50 inner, 24 outer)
- Inner array:
  - f_1 = 40 kHz, l_1=1
- Outer array:
  - f_2 = 41 kHz, l_1=2
- Focal:
  - F = 100 mm



Methods

Linear field calculation

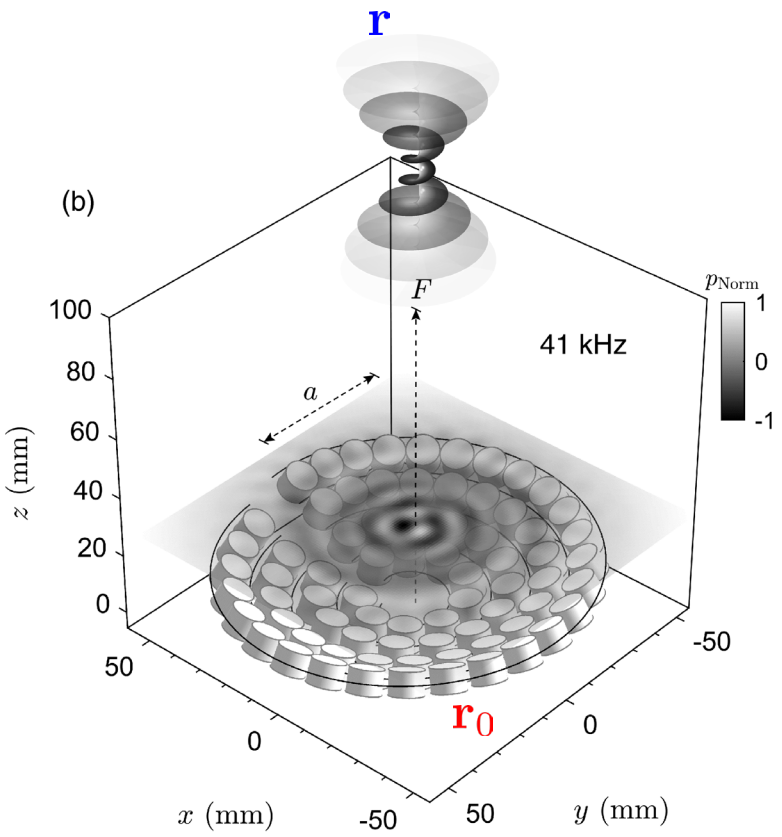
- Rayleigh integral

$$p(\mathbf{r}, \omega_n) = -i\frac{\rho_0 c_0 k_n}{2\pi}\int_{S_0}\frac{v_0(\mathbf{r_0})\exp(ik_n\,|\mathbf{r}-\mathbf{r_0}|)}{|\mathbf{r}-\mathbf{r_0}|}dS_0,$$

- where ρ_0 is the density, the c_0 is sound speed, $k_n = \omega_n/c_0$ the wavenumber for the n-th source, and $v_0(\mathbf{r}_0)$ the velocity normal to the surface S_0.

Solution

- Integration for each piezoelectric source (circular disc),
- To the desired point in the space,
- Integration at the exit plane is used for nonlinear simulations.



Methods

Nonlinear field calculation

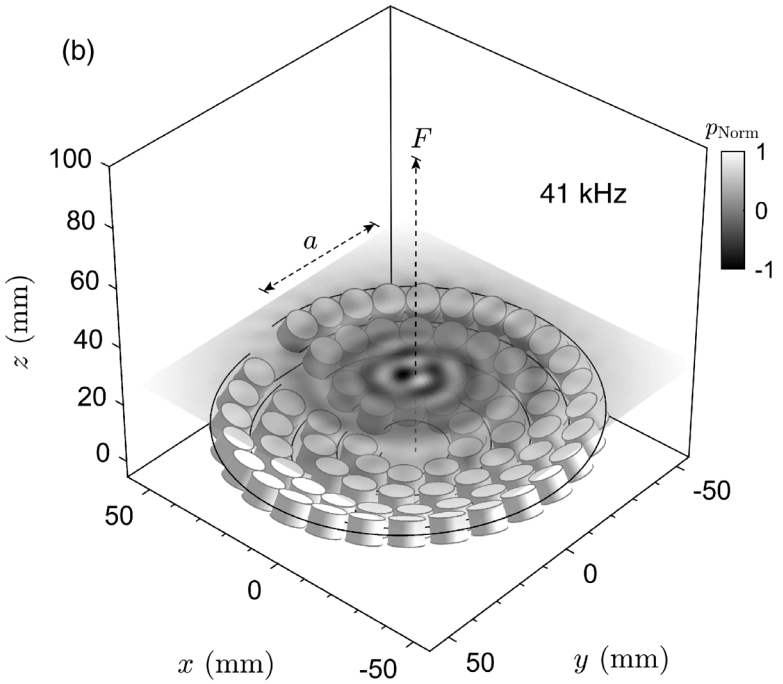
- One-way Westervelt equation [1, 2]

$$\frac{\partial^2 p}{\partial \tau \partial z} = \frac{c_0}{2}\nabla^2 p + \frac{\beta}{2\rho_0 c_0^3}\frac{\partial^2 p^2}{\partial \tau^2} + \frac{b}{2\rho_0 c_0^3}\frac{\partial^3 p}{\partial \tau^3},$$

- where p is the acoustic pressure, β is the coefficient of nonlinearity, b the thermoviscous absorption coefficient

Solution

- Operator-splitting: for a small axial distance Δz, the pressure in a retarded frame $\tau = t - z/c_0$ is calculated splitting the physical terms:
- Diffraction: $\frac{\partial p}{\partial z} = \int \frac{c_0}{2}\nabla^2 p \, d\tau,$ [k-space, angular spectrum]
- Nonlinearity: $\frac{\partial p}{\partial z} = \frac{\beta}{2\rho_0 c_0^3}\frac{\partial p^2}{\partial \tau},$ [frequency domain, RK]
- Absorption: $\frac{\partial p}{\partial z} = \frac{b}{2\rho_0 c_0^3}\frac{\partial^2 p}{\partial \tau^2}$ [frequency domain]



[1] Westervelt, JASA 35(4) 535–537 (1963)
[2] P. Yuldashev et al. Acoust. Phys. 57, 334 (2011).

Results

Generation process

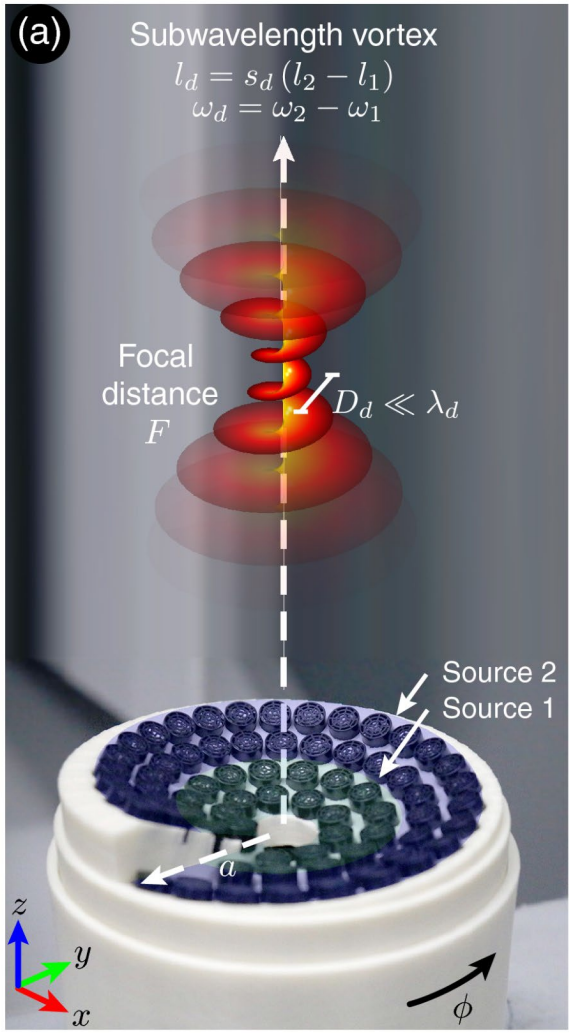
- Homogeneous media present very-weak dispersion.
- Harmonics generate locally and accumulate with distance.
- Self-demodulated component should present, in the near field, a similar pressure distribution than the primary beams.
- The self-demodulated component depends on the spatio-temporal interference of the two primary vortex beams.
- Linked to their detuning frequency and their topological charges.

Self-demodulated vortices

- Self demodulated beam present a phase $\exp(il_d\phi)$
- The topological charge of the self-demodulated vortex is*

$$l_d = \mathrm{sign}(\omega_2 - \omega_1)(l_2 - l_1)$$

*due to the conservation of angular momentum during nonlinear mixing

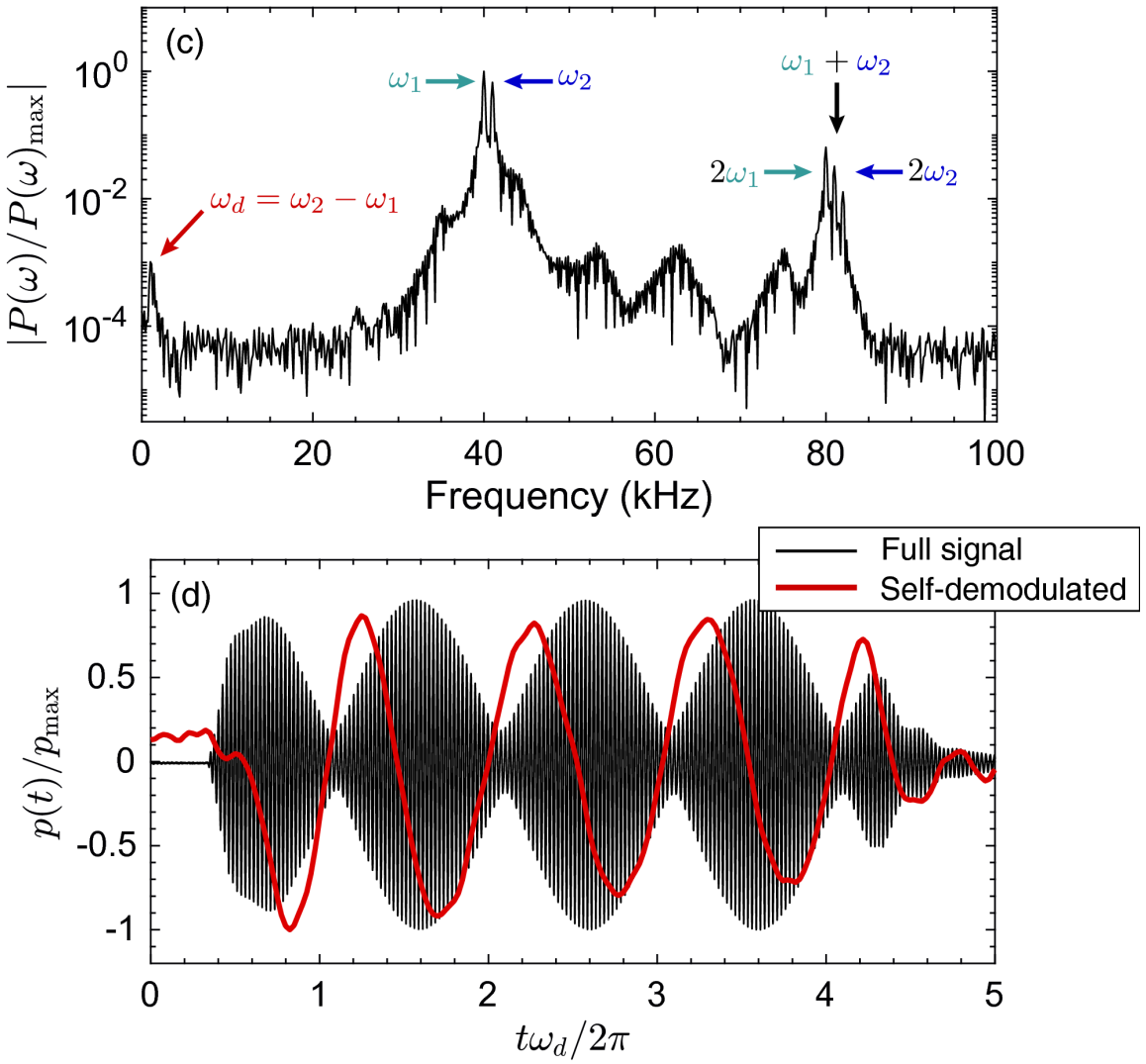


JL Thomas and R. Marchiano, PRL 91 244302 (2003)

Results

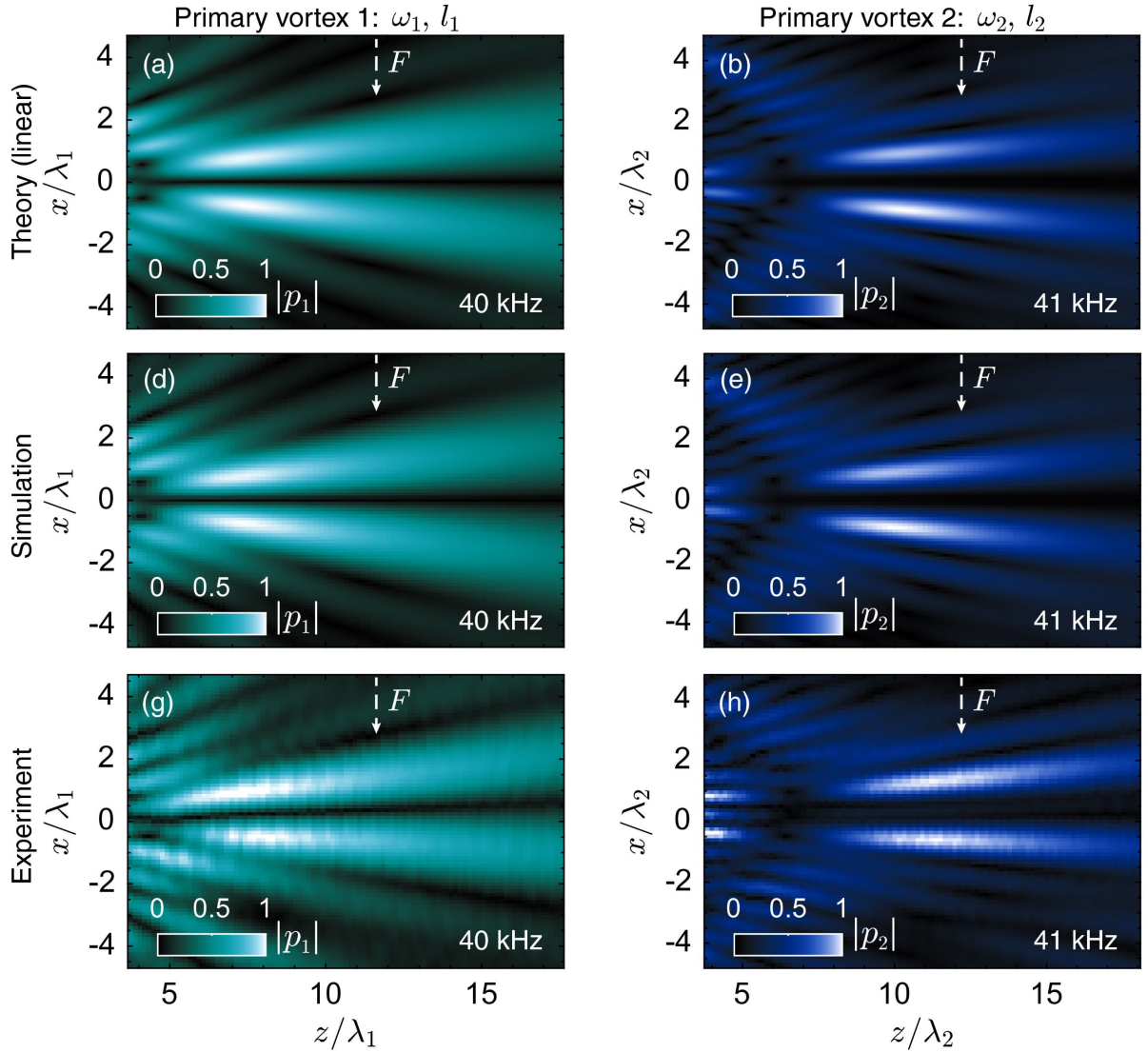
Self-demodulation

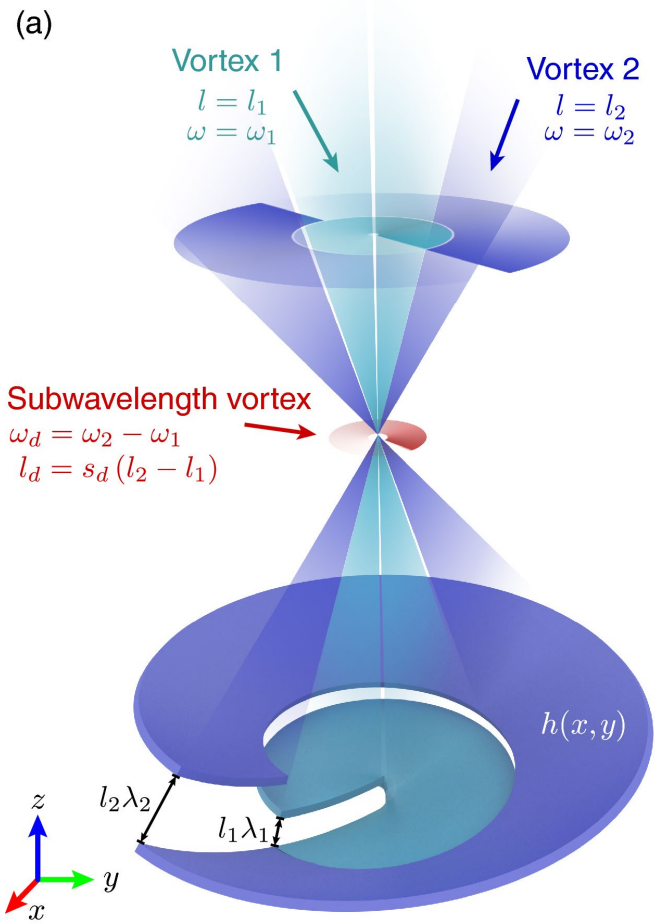
- The maximum pressure amplitude was 16,1 Pa (118,1 dB SPL).
- At 40 kHz and in air, nonlinear effects are triggered.
- Higher and difference frequency harmonics arise as arithmetical combinations of the primary components
- In addition to higher harmonics, a difference-frequency mode, of frequency $\omega_d = \omega_2 - \omega_1$ is generated due to the nonlinear self-demodulation of the beating waveform



Results

Subwavelength vortices





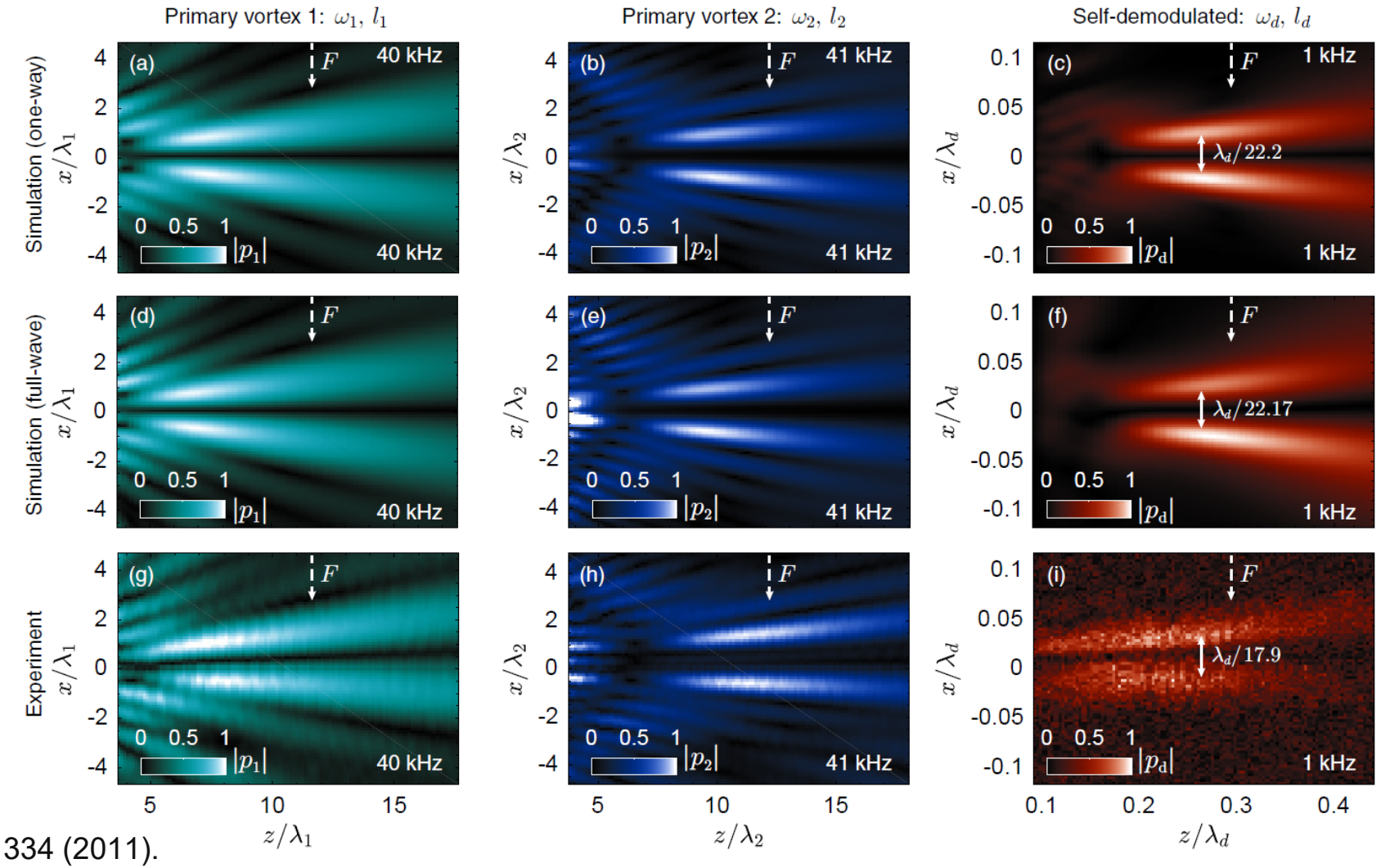
Results

Subwavelength vortices

One-way Westervelt [1]
Operator splitting +RS near field

Full wave simulations [2]
Pseudospectral time domain (k-wave)

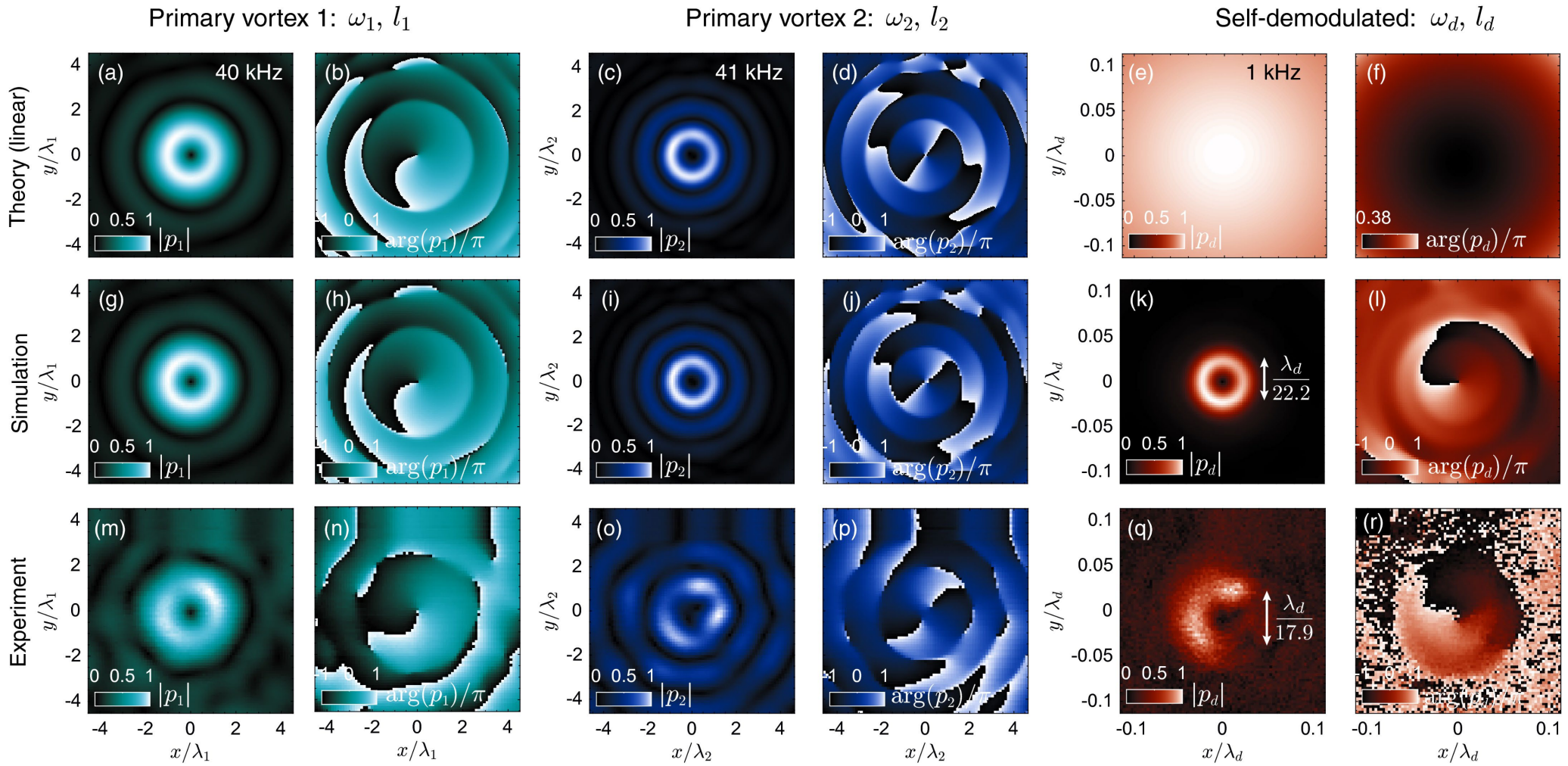
Experiments
Hydrophone in water tank



[1] P. Yuldashev et al. Acoust. Phys. 57, 334 (2011).
[2] B. Treeby, et al. JASA 131.6 4324-4336 (2012)

Results

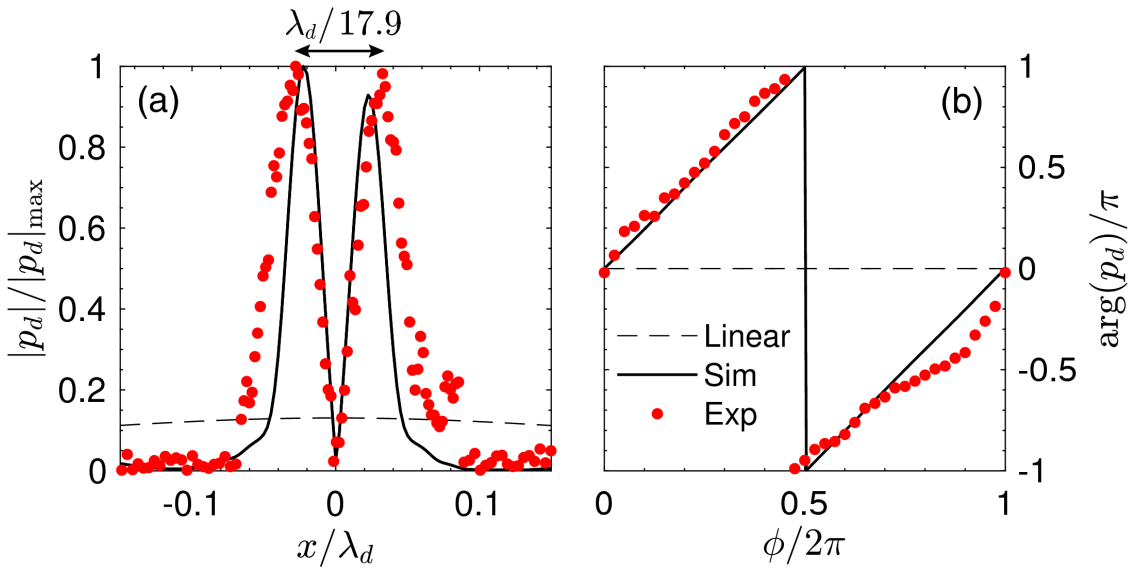
Subwavelength vortices



Results

Subwavelength vortices

- The width of the vortex is smaller than the wavelength
  - 17,9 times smaller in experiments
  - 22,2 times smaller in simulations
- The measurement distance was 2,8 times the Rayleigh diffraction length
- The phase of the beam along the azimuthal coordinate agrees with $l_d\phi$
- The topological charge is $l_d = \mathrm{sign}(\omega_2 - \omega_1)(l_2 - l_1)$: Angular momentum during nonlinear mixing is conserved

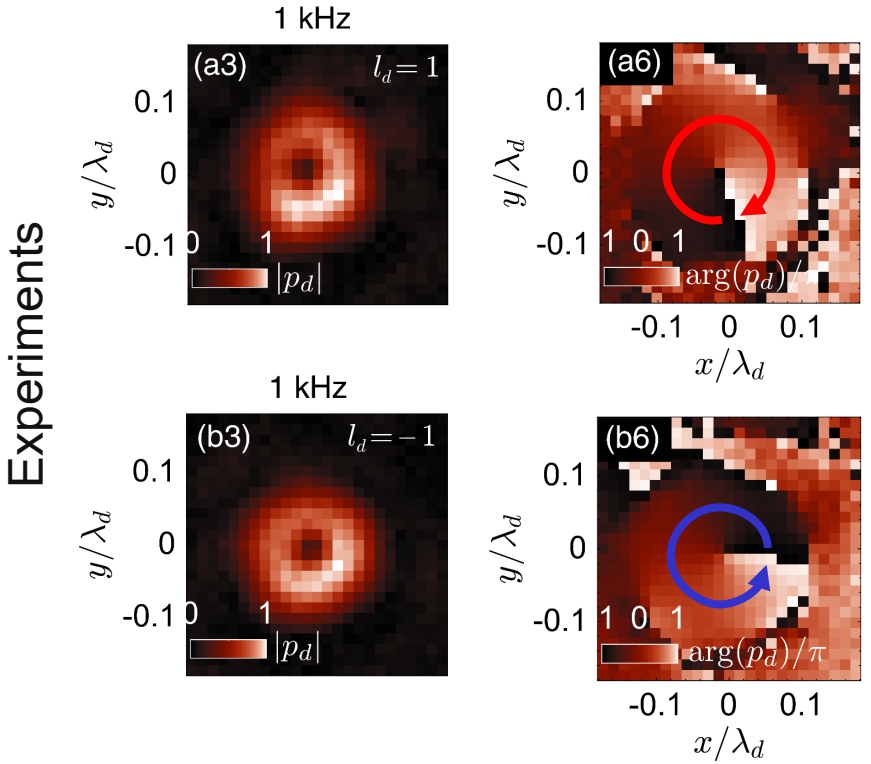


Results

Subwavelength vortices

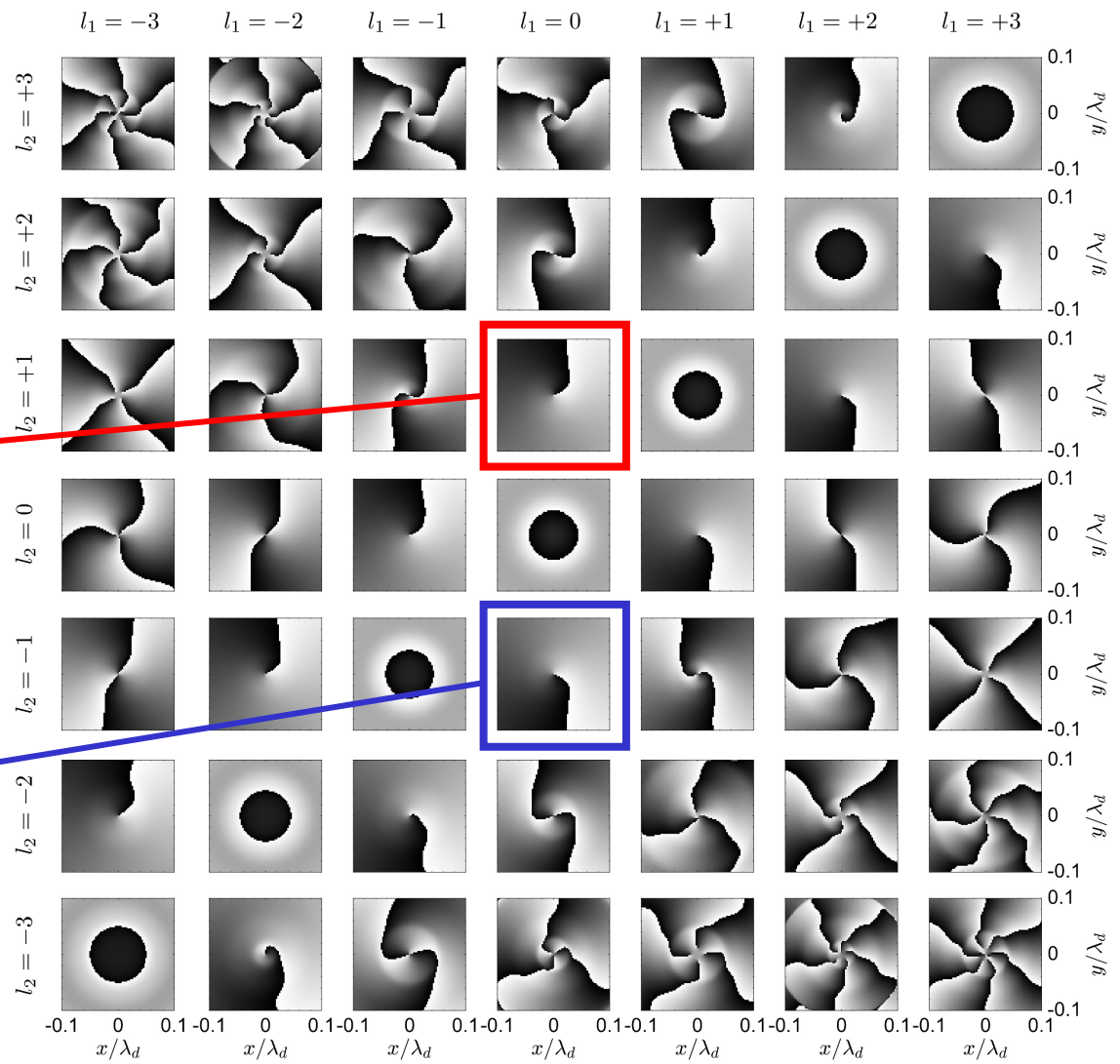
- Any combination results in a subwavelength vortex

$$l_d = \mathrm{sign}(\omega_2 - \omega_1)(l_2 - l_1)$$



$l_d = 1 - 0 = 1$

$l_d = 0 - 1 = -1$



Conclusions

Subwavelength vortices

- By using nonlinearity, **vortices smaller than the wavelength are generated** (*parametric vortex antenna*)
- Pressure distribution is linked to the spatiotemporal interference of the two primary beams
- Subwavelength vortices emerge due to the conservation of angular momentum during nonlinear mixing

Conditions

- The primary beams should present different topological charges and frequencies
- The field if the primary beams should overlap in space

Applications

- Long-range transceivers / acoustic modems / parametric arrays
  - Once generated, they should maintain the directivity of the primary beams, as in end-fire arrays parametric antennas
- Acoustic radiation force / tweezers
  - Once generated by a high-frequency beams, they can propagate longer in absorbing media

More details in …

- N Jiménez, J Ealo, RD Muelas-Hurtado, A Duclos, V Romero-García. Sub-wavelength acoustical vortex beams using self-demodulation. Physical Review Applied, 15 (5), pp. 054027, (2021)

Acknowledgements

Funding

- **Spanish Ministry of Science and Universities**: IJC2018-037897-I, Juan de la Cierva – Incorporación,
- **Agència Valenciana de la Innovació**: INVA1/2020/92, INNCON/2020/009
- **Pays Région de la Loire**: HIPERMETA project
- **European Union**: COST Action DENORMS CA15125,

COST is supported by the EU Framework Programme Horizon 2020

Thanks for your attention!